New Forests (2025) 56:13
https://doi.org/10.1007/s11056-024-10081-7

RESEARCH

Shrub aboveground biomass estimation considering bulk volume geometry: general and specific models for 14 species in the Mediterranean central Chile

Erico Kutchartt[1,2] · Jorge Gayoso[3] · Javier Guerra[4] · Francesco Pirotti[2] · Daniele Castagneri[2] · Radim Matula[5] · Yasna Rojas[6] · Mark E. Olson[7] · Martin Zwanzig[8]

Received: 26 April 2023 / Accepted: 18 November 2024 / Published online: 28 November 2024

Abstract
Shrubland ecosystems cover a large part of the five Mediterranean regions of the world, and monitoring their biomass is crucial for assessing fire risk and carbon sequestration. However, biomass models for multi-stemmed shrubs remain scarce, making the quantitative assessment of shrubland biomass imprecise and often unreliable. Here, we measured, harvested, and weighed 411 specimens at two representative sites to quantify aboveground biomass (AGB) in 14 shrub species. To develop species-specific and general models of AGB, we used observations on total height (HT), diameter at collar height (DCH), number of stems (NS), and crown size as well as different geometric shapes representing crown area (CA) and bulk volume (BV). General models including all species were fit, including species identity as a random effect to take variation across species into account. A k-fold cross-validation was used to assess and compare the ability of the models to predict independent data. Individual AGB varied markedly both within and among the 14 species, with on average higher values at the site characterized by lower shrub density and species richness. Two biomass components, woody and leaf + twig, were distinguished, and species-specific means of the woody and leaf + twig proportion varied between 30 and 60%. We found that crown BV assessed on different geometric shapes was suitable to predict the biomass for different shrub species and that additional variables were rarely beneficial. The best general model included BV represented as an inverted truncated cone, derived from crown diameter (CD), HT and the DCH of the longest stem. This study provides novel allometric equations essential for assessing AGB shrublands in central Chile. Our general multi-species models based on BV geometry could prove very useful for future studies in Mediterranean shrublands, allowing us to estimate biomass through indirect, non-destructive methods.

Keywords Biomass model · Allometric equations · Biomass allocation · Crown dimensions · Mediterranean shrubland

Extended author information available on the last page of the article

Introduction

Mediterranean shrubland globally covers $2.8 \cdot 10^6$ km^2 (Chapin et al. 2011) within five Mediterranean zones (the Mediterranean basin, California, central Chile, the western Cape of South Africa, and southwest and south Australia), which are referred to by different terms, such as Chaparral (USA), Matorral (Chile), Fynbos (South Africa), or Garrigue (the Mediterranean basin) (Cowling et al. 1996; Sağlam et al. 2008). These ecosystems are characterized by a highly diverse array of (mostly) evergreen and drought-resistant shrubs adapted to the region's hot, dry summers and mild, rainy winters (Médail and Quézel 1999; Cowling et al. 2015). The importance of Mediterranean shrubland on a global scale includes carbon sequestration and biodiversity conservation, prevention of soil erosion and desertification, water storage, catalyzing nutrient cycles, and climate change mitigation (Conti and Díaz 2013; Gratani et al. 2013; Ruiz-Peinado et al. 2013; Pasalodos-Tato et al. 2015; Madrigal-González et al. 2023). In Chile, Mediterranean shrubland is represented by the sclerophyllous type of vegetation and covers 1.5 Mha (INFOR 2022). It is classified as one of the 25 biodiversity hotspots in the world due to its high endemism and, as a consequence, is designated for conservation priority (Myers et al. 2000). Despite the great importance of this ecosystem, Mediterranean shrubland has suffered multiple anthropogenic disturbances since Euro-Chilean settlement, such as urban expansion, forest fires, agricultural expansion, logging for firewood, and over-grazing from livestock, all of which have substantially reduced its extent (Schulz et al. 2011; Smith-Ramírez et al. 2023).

Allometric equations are fundamental for the biomass and carbon stock quantification of Mediterranean shrubland, which are important inputs within the Kyoto Protocol agreement and the implementation of REDD + initiatives under the UNFCCC (Nyamukuru et al. 2023). A few studies have developed allometric equations to estimate the aboveground biomass (AGB) in shrub species in different regions using crown attributes (e.g., Vora 1988; Usó et al. 1997; Paton et al. 2002; Huff et al. 2017). In Chile, biomass equations have been created mostly for large native tree species (e.g., Caldentey 1995; Kutchartt et al. 2021), but scant information is available for multi-stemmed shrubs (Orrego 2014; Cruz et al. 2015). This lack of information makes it difficult to estimate AGB in shrubs using indirect methods, either using species-specific models or general models. The advantage of general models is that they obviate the need for species identification, making them useful for remote sensing applications, especially combining models based on crown area (CA) at individual tree level with aerial photographs, drone-flight, or airborne laser scanning data (Menéndez Miguélez et al. 2022). However, species-specific models are expected to provide more accurate estimates of biomass than generic models (Buech and Rugg 1989; Sah et al. 2004; Paul et al. 2013; Annighofer et al. 2016). Similarly, information regarding biomass allocation (e.g., woody biomass, leaves, twigs, roots, etc.) is poor in the shrub biomass literature. Separating biomass allocation is particularly important in Mediterranean shrubland because different biomass fractions are affected differently by fire in this fire-mediated ecosystem (e.g., Papió and Trabaud 1990), but also for other ecological considerations, such as the soil nutrient status, or browsing by livestock (Peichl and Arain 2007).

Shrub biomass can be modelled through classic allometric relationships between weight and diameter at breast height (DBH) (Cruz et al. 2015). However, the architecture of shrubs is different from that of trees (Yao et al. 2021). Shrubs do not have a single stem, and selecting one out of many to estimate the entire plant biomass is often not appropriate due to the difficulty of obtaining an accurate stem diameter for a multi-stemmed plant (Zeng et al. 2010). Even measuring the diameters of all the stems (Matula et al. 2015) or

the thickest one in an individual does not necessarily allow for correctly assessing woody biomass (Northup et al. 2005). Thus, other covariables have been proposed in the literature. Measuring length and diameter of the canopy allows computing its CA or bulk volume (BV), which are useful covariables to estimate AGB in shrubs (Ludwig et al. 1975; Návar et al. 2004; Ali et al. 2015; Yao et al. 2021). These can be easily measured in the field or through remote sensing. Different authors, such as Ludwig et al. (1975), Murray and Jacobson (1982), Usó et al. (1997), and Conti et al. (2013), have proposed several geometric shape approaches to assess the CA and BV of the crown to predict AGB, which could be more beneficial instead of measuring the stem diameter in some specific shrubs. Other explanatory variables such as total height (HT), number of stems (NS), age, wood density (WD), or stem diameter at different heights can improve biomass models in addition to crown size and shape (Chave et al. 2005; Alvarez et al. 2012; Conti et al. 2013; Ali et al. 2015; Huang et al. 2022; Kouamé et al. 2022). All in all, the inclusion of robust allometric equations for shrub species in a national database is an important input to improving forest inventories and carbon stock quantification, especially because of constant anthropogenic disturbances to this fragile ecosystem. Hence, robust biomass equations are essential to be able to quantify the carbon capture ability of new and restored shrublands.

In this study, we aimed to (1) develop species-specific and general AGB models for 14 dominant shrub species in the sclerophyllous Mediterranean shrubland of central Chile, (2) test predictive variables using geometric shapes of the crown, such as different crown projection areas and bulk volumes, and examine whether variables additional to the main predictor variable improve the models, and (3) determine biomass allocation between woody and leaf + twig biomass in the species studied.

Material and methods

Study area

The study was conducted at two representative sites of arborescent shrub species at mature stage in the Mediterranean ecosystem of the O'Higgins region in central Chile (Lübert and Pliscoff 2018; Miranda 2022). One site was located at Cortaderal (34°35′S 71°29′W) and the other site at Miraflores (34°08′S 70°37′W) (Fig. 1). The cover vegetation differed between sites. Cortaderal was arborescent, semi-dense (50–75%) to dense (> 75%), with abundant herbaceous vegetation and shrub regrowth, while Miraflores was semi-dense to open (25–50%), with little herbaceous vegetation and sparse recent woody growth. The vegetation cover among open and semi-dense areas represents 32% and 35% of the shrubland area, respectively (CONAF 2021), and corresponds to sites that have been heavily intervened during the last two centuries. In the last 40–50 years, there has been a process of natural recovery of native sclerophyllous vegetation, although sporadic grazing persists (Schulz et al. 2010). Temperatures are higher at Miraflores than Cortaderal, with a mean temperature of 16.3 °C in Miraflores compared to 12.0 °C in Cortaderal. The estimated mean annual precipitation is slightly higher at Cortaderal with 725 mm, compared to the 688 mm in Miraflores, which represent a steep area, which is much more pronounced compared to Cortaderal sector (Kutchartt et al. 2022). In general, both Cortaderal and Miraflores have marked dry seasons (Fick and Hijmans 2017). The soils at the Cortaderal are moderately deep, on andesitic rocks and diorites with different degrees of weathering. The texture is characterized by silty clay loam at the surface and clayey loam at depth, with

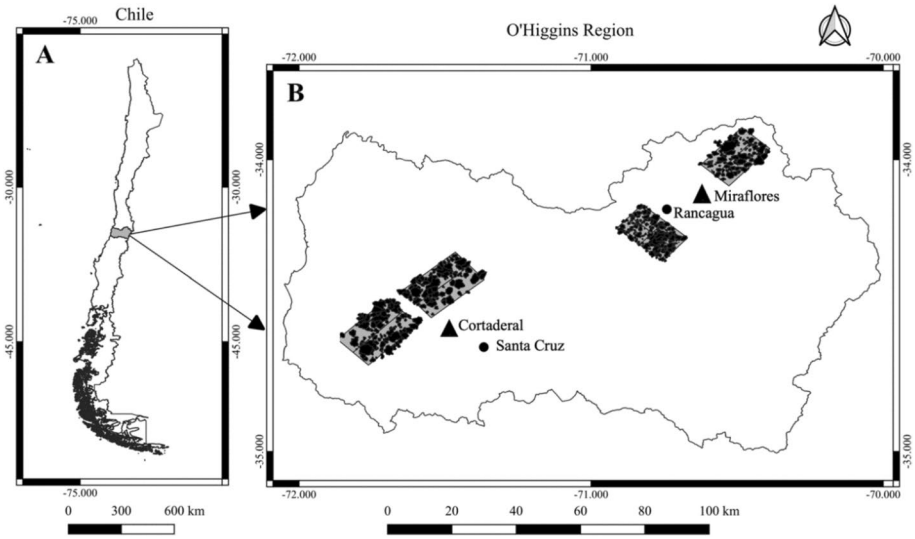

Fig. 1 Study area. **A** Location of the O'Higgins region within the Republic of Chile **B** The triangles indicate the Cortaderal and Miraflores sites and in circles the cities of Santa Cruz and Rancagua, central Chile

organic carbon content decreasing with depth, with 4.4% at 0–12 cm, 2.4% at 12–28 cm, and 1.5% at 28–50. The soils at Miraflores vary from 20 to 70 cm in depth, with a rocky substrate appearing at 42 cm. The thin soil was formed from eruptive rocks containing dioritic and porphyritic rocks with little to moderate weathering. Slight to moderate stoniness was found on the surface, with occasional rocky outcrops. The texture is silty clay loam at the surface and clay loam at depth. The organic carbon decreases from 1.8% at 0–16 cm to 0.8% at 16–42 cm (CIREN 1996).

Field data collection

During the summer of 2018, 411 shrubs of 14 species were sampled at the two sites (two plots of 1,000 m^2 at each site; see Table 1). The shrubs within the plots were measured, harvested and weighed. The recorded attributes were DCH (identifying the longest stem as a representative one), measured with a calliper; *crown diameter* (CD; values between the two-perpendicular axis, north- and east-oriented); *crown length* (CL); and HT; measured with a measuring tape; and the NS, which were counted (Table 1). After the shrubs were harvested, *woody biomass* (WB) and *leaf+twig biomass* (LTB) were separated and weighed fresh for each entire shrub in the field using a digital scale with a 100 kg capacity and a graduation of 100 g to get only the component fractions. Leaves and twigs < 1 cm in diameter were considered a single component in order to simplify the fieldwork (e.g., Wang and Niu 2016). For *Podanthus mitiqui* and *Retanilla trinervia*, WB was not separated from LTB because a significant part of its foliage had fallen at the time of sampling. Thus, for these two species, we only computed the total AGB and were unable to weigh the leaf fraction (see Table 1). Finally, samples for WD and *moisture content* (MC) determination were collected at 0.3 m aboveground and measured

Table 1 Mean and standard deviations of the main attributes of the 14 shrub species from the O'Higgins region in central zone Chile, at two sites (2000 m^2 of area of sampling in each site)

Species (Scientific name)	Common name	n	DCH (cm)	CD (m)	CL (m)	HT (m)	NS (n)	WB (kg)	LTB (kg)	AGB (kg)
Cortaderal site										
Aristotelia chilensis (Mol.) Stuntz	Maqui	22	3.6 ± 2.2	1.8 ± 0.8	1.9 ± 0.9	2.6 ± 0.9	4.4 ± 2.9	2.10 ± 1.97	1.24 ± 1.19	3.31 ± 2.91
Azara dentata Ruiz & Pavon	Corcolen	51	4.7 ± 2.5	1.5 ± 0.7	1.6 ± 0.7	2.2 ± 0.9	4.4 ± 4.3	2.77 ± 4.05	1.56 ± 1.49	4.34 ± 5.10
Baccharis linearis (Ruiz & Pav.) Pers	Romerillo	42	4.2 ± 2.8	1.0 ± 0.7	1.1 ± 0.4	1.6 ± 0.6	3.7 ± 3.8	1.66 ± 2.56	0.46 ± 0.50	2.13 ± 2.95
Baccharis macraei Hook. & Arn	Vautro	26	2.4 ± 0.7	1.5 ± 0.5	1.4 ± 0.4	1.5 ± 0.4	4.8 ± 3.1	0.68 ± 0.63	1.15 ± 1.14	2.22 ± 1.96
Berberis horrida Gay (Michay)	Michay	20	1.5 ± 0.6	0.9 ± 0.3	1.3 ± 0.5	1.5 ± 0.5	4.4 ± 2.1	0.25 ± 0.21	0.23 ± 0.19	0.48 ± 0.39
Escallonia pulverulenta (Ruiz et Pav.) Pers	Corontillo	30	4.0 ± 2.6	1.2 ± 0.7	1.6 ± 0.8	2.6 ± 0.9	2.8 ± 2.5	1.77 ± 2.09	0.83 ± 0.91	2.52 ± 2.82
Gochnatia foliosa D.Don (Mira Mira)	Mira Mira	27	3.4 ± 1.7	1.9 ± 0.8	1.5 ± 0.6	2.0 ± 0.6	10.1 ± 7.2	3.36 ± 3.99	1.97 ± 2.00	5.32 ± 5.82
Kageneckia oblonga Ruiz et Pav	Bollen	26	4.1 ± 2.2	1.1 ± 0.6	1.5 ± 0.7	2.7 ± 1.0	1.3 ± 0.5	2.08 ± 2.35	0.86 ± 0.75	2.93 ± 2.87
Lomatia hirsuta (Lam.) Diels ex J.F.Macbr	Radal	20	4.9 ± 1.9	1.6 ± 0.3	2.7 ± 0.8	3.5 ± 1.1	2.7 ± 3.1	2.59 ± 1.44	1.19 ± 0.52	3.78 ± 1.79
Myrceugenia obtusa (DC.) O.Berg	Arrayancillo	24	5.9 ± 3.5	1.7 ± 0.9	1.8 ± 0.7	2.2 ± 0.8	5.7 ± 4.8	5.46 ± 5.72	3.15 ± 2.74	8.60 ± 8.28
Teucrium bicolor Sm	Oreganillo	27	0.6 ± 0.3	0.5 ± 0.2	0.7 ± 0.2	0.9 ± 0.2	6.3 ± 3.0	0.05 ± 0.03	0.04 ± 0.02	0.10 ± 0.04
Cortaderal site		315	3.7 ± 2.6	1.3 ± 0.8	1.5 ± 0.8	2.1 ± 1.0	4.6 ± 4.3	2.16 ± 3.25	1.17 ± 1.51	3.27 ± 4.47
Miraflores site										
**Baccharis linearis* (Ruiz & Pav.) Pers	Romerillo	25	3.5 ± 1.8	1.5 ± 0.7	1.1 ± 0.4	1.5 ± 0.5	5.6 ± 4.0	3.38 ± 4.04	1.05 ± 0.67	4.43 ± 4.63
Colliguaja salicifolia Gillies & Hook	Colliguay	29	3.4 ± 1.3	2.3 ± 0.9	1.3 ± 0.4	1.7 ± 0.5	12.8 ± 7.3	6.20 ± 7.41	4.33 ± 3.62	10.54 ± 10.13
***Podanthus mitiqui* Lindl	Mitiqui	22	2.3 ± 1.2	1.7 ± 0.6	1.7 ± 0.5	1.8 ± 0.5	10.8 ± 6.8	-	-	2.73 ± 1.91
***Retanilla trinervia* (Gillies & Hook.) Hook. & Arn	Tevo	20	6.3 ± 2.5	3.4 ± 1.3	2.6 ± 0.8	2.8 ± 0.8	7.4 ± 3.7	-	-	19.25 ± 11.00
Miraflores site		96	3.8 ± 2.2	2.2 ± 1.1	1.6 ± 0.7	1.9 ± 0.7	9.3 ± 6.4	4.90 ± 6.20	2.81 ± 3.14	8.97 ± 9.90

n = *number of shrubs sampled by species*, DCH = *diameter at collar height* (cm), CD = *crown diameter* (the mean value between x and y axis; m), CL = *crown length* (m), HT = *total height* (m), NS = *number of stems*, WB = *woody biomass* (kg), LTB = *leaf* + *twig biomass* (kg), AGB = *aboveground biomass* (kg)

**Baccharis linearis* (Ruiz & Pav.) Pers. was presented in both sites and the dataset was divided into two groups according to the site because it was necessary for extract the mean values and standard deviation of the variables by site

**It was not possible divide between these two biomass components (woody and leave + twig biomass) in the field for *P. mitiqui* and *R. trinervia* due the lack of leaves and twigs (< 1 cm)

using a piece of stem in the laboratory to calculate the dry weight of each shrub (see more details in Kutchartt et al. 2022).

Crown area and bulk volume

From the field data, additional dimensions were calculated to characterize the crown areas and volumes of the shrubs. CA was computed as both a circle (1) and an ellipse (2) and later used as a covariate for model-based prediction of AGB.

$$CAc = \frac{\pi}{4} \cdot \left(\frac{CD_x + CD_y}{2} \right)^2 \tag{1}$$

$$CAe = \frac{\pi}{4} \cdot \left(CD_x \cdot CD_y \right) \tag{2}$$

where CA_c is the *crown area* of a circle and CA_e is the *crown area* of an ellipse in m^2, CD_x is the *crown diameter* on the x-axis, and CD_y is the *crown diameter* on the y-axis (perpendicular to the x-axis) in m.

In addition to computing CA_c and CA_e, DCH, CL and HT were used to calculate the volumes of the crown and of the entire shrub (e.g., Tian et al. 2014). The shrub crown was depicted by a solid of revolution corresponding to the most common species. We used the volume of six geometric shapes in total. In the case of an elliptical cone and hemi-sphere, both HT and CL have been used to determine volume. The other two geometric figures were referred to as the inverted truncated cone and elliptical cube, with the aim of exploring which geometric figure could best fit the actual crown of the shrubs studied (Fig. 2). Hereafter, the volume of each geometric shape was also tested as a covariate in our modelling fits. The volume we calculated was BV, also known as apparent biovolume (m^3), which refers to the specific body of the plant (e.g., Blanco Oyonarte and Navarro Cerrillo 2003). Therefore, the crown volume will be defined as the BV hereafter.

Biomass modelling

Basic shrub attributes such as DCH, HT, NS and CD were plotted to analyse their general and species-specific relationships (Fig. 3), and to understand if and how the diverse architectural shapes of the shrubs needed to be considered for modelling purposes. Shrub AGB was modelled using the mathematical expression $y = aX^b$ (e.g., Zianis and Mencuccini 2004) and derivates of this form to check whether adding more covariables improved the model's fit and predictive ability (e.g., Conti et al. 2019). Either DCH, CA, or BV were selected as the main predictor variables, and HT and NS were additional variables for the species-specific models. In total, we formulated thirteen models (Eqs. 3–13), some of which received different inputs for CA and BV.

$$Y = \beta_0 DCH^{\beta_1} \tag{3}$$

$$Y = \beta_0 \left(DCH^2 \right)^{\beta_1} \tag{4}$$

$$Y = \beta_0 DCH^{\beta_1} HT^{\beta_2} \tag{5}$$

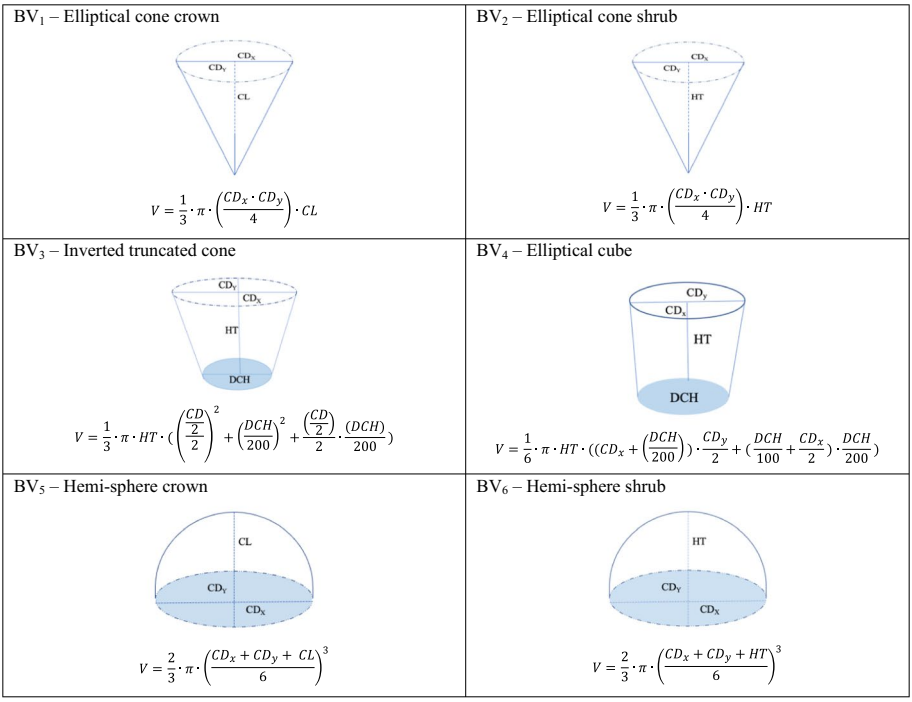

Fig. 2 Geometric shapes used to calculate different crown BV that were included as variables in the total AGB models. Where BV_i is the *bulk volume* referring to the specific geometric shapes, DCH is the *diameter at collar height*, HT is the *total height*, CD_x is the *crown diameter* north–south axis, CD_y is the *crown diameter* west–east axis, CD is the mean value between CD_x and CD_y and CL is the *crown length*

$$Y = \beta_0 DCH^{\beta_1} HT^{\beta_2} NS^{\beta_3} \tag{6}$$

$$Y = \beta_0 CA_x^{\beta_1} \tag{7}$$

$$Y = \beta_0 CA_x^{\beta_1} HT^{\beta_2} \tag{8}$$

$$Y = \beta_0 CA_x^{\beta_1} HT^{\beta_2} NS^{\beta_3} \tag{9}$$

$$Y = \beta_0 BV_x^{\beta_1} \tag{10}$$

$$Y = \beta_0 BV_x^{\beta_1} HT^{\beta_2} \tag{11}$$

$$Y = \beta_0 BV_x^{\beta_1} HT^{\beta_2} NS^{\beta_3} \tag{12}$$

$$Y = \beta_0 \left(DCH^2 HT\right)^{\beta_1} \tag{13}$$

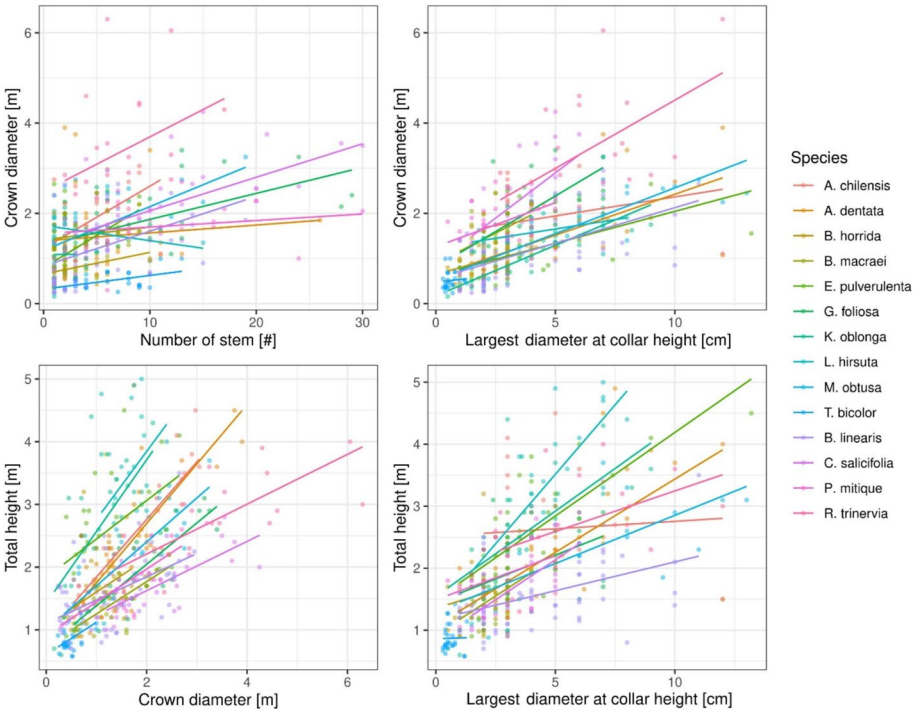

Fig. 3 General and species-specific relationships of basic shrub attributes: NS vs. CD (top left), largest DCH vs. CD (top right), CD vs. HT (bottom left) and largest DCH vs. HT (bottom right). The lines refer to simple linear models fitted to the data of each species. Crossing lines indicate interaction effects mediated by species, e.g., a strong, species-specific difference in the degree of interaction of the variables (compare slope differences) or even negative instead of positive relations (only given the NS vs. CD (*K. oblonga*))

where DCH is the *diameter at collar height* in cm, CA is the *crown area* in m^2, the subscript (x) refers to circle (c) or ellipse (e), BV is the *bulk volume* in m^3, and the subscript designates one of six geometric shapes used as a covariate in the model (Fig. 2), HT is the *total height* in m, and NS is the *number of stems*.

Because two approaches were used for calculating CA, Eqs. 7, 8, and 9 actually represent six different models. Similarly, six different geometric shapes were used to compute BV (Fig. 2), increasing the number of models derived from Eqs. 10, 11, and 12 from three to eighteen. In total, twenty-nine models were tested for each of the 14 shrub species to identify the best species-specific biomass model.

In addition, we developed linear mixed effects models, considering independent variables such as CA, or BV, or derivates of DCH as a single explanatory variable and species as a random effect, to identify the best simple general shrub biomass model. Taking into account different variances per species (Tischer et al. 2020), random intercept and slope models were fitted by maximum likelihood (ML), resulting in unbiased estimates for the general intercept and slope parameters. The ML approach stands for a parameter estimation procedure that makes the observations most probable and allows a comparison between models.

Model selection criteria and validation methods

The main criterion to compare the models was their ability to reliably predict data to which they were not fitted. Because the number of observations per species was relatively low and independent data were not available, the data at hand were repeatedly used to perform k-fold cross-validation. For this approach, the data were split into five folds (subsets): four as training data (model fitting) and one for testing (comparing model predictions with real observations). For a single k-fold cross-validation, each of the folds was used once for testing and the others for training. In a repeated k-fold cross-validation, the sampling of the data into folds is repeated. Here we performed 1,000 repetitions of each fivefold cross-validation and evaluated the model based on its ability to predict the testing data points, which accounted for 20% of the total data in each of the 5,000 evaluation steps. To correct the bias when the predicted data were transformed from a logarithmic scale back to the original scale, the correction factor (CF) by Baskerville (1972) was calculated and used for each step.

$$CF = e\left(\frac{SEE^2}{2}\right) \tag{14}$$

where CF is the *correction factor*, e is the *exponent*, and the SEE is the *standard error of the estimation*. Correction factors were thus calculated for each model and will be reported along with the best model equations and their parameters, so that corrected response variables can be calculated by multiplying the result of the given equation with the respective CF.

To evaluate and compare tested models, several performance criteria for assessing were calculated as arithmetic mean of the criteria computed for each of the step of the k-fold cross-validation. A number of criteria were used to compare the performance of the models tested. The *root mean square error* (RMSE, kg; Eq. 15), the *mean absolute percentage error* (MAPE, %; Eq. 16), and the *coefficient of determination* (R^2; Eq. 17) were used to evaluate the goodness-of-fit, in particular of all species-specific models fitted with ordinary least squares regression. To select the best model, the RMSE based on a repeated k-fold cross-validation (CV-based) was used to rank the models in order to avoid selecting overfitted models. Models were considered to be indistinguishable by RMSE, when their estimated RMSE was lower than a threshold defined by the lowest RMSE plus two times its standard deviation. These models were in addition compared by the *percent relative standard error* (PRSE, %; Eq. 18) of their parameter estimates to check the uncertainty in each parameter, finally representing an evaluation similar to the scheme of the Akaike information criterion (AIC; Eq. 19). For the PRSE comparison, the maximum PRSE of each model was derived from all parameters associated with a covariate, i.e. expect the intercept. The exclusion of the intercept in this evaluation was applied to avoid that intercepts estimated to be around zero, and which are therefore not important, but still show some uncertainty in determination, will inflate the maximum PRSE used for this model ranking in the second step. While the CV-based RMSE – PRSE evaluation was used for the species-specific models, the AIC was used as the primary evaluation criterion for the general models, which were fitted by maximum likelihood and where the best model was identified as the one with the lowest AIC.

$$RMSE = \sqrt{\frac{1}{n}\sum_{i=1}^{n}\left(y_i - \hat{y}_i\right)^2} \tag{15}$$

$$MAPE = \frac{100}{n}\sum\frac{\left|\hat{y}_i - y_i\right|}{y_i} \tag{16}$$

$$R^2 = 1 - \frac{\sum_{i=1}^{n}\left(y_i - \hat{y}_i\right)^2}{\sum_{i=1}^{n}\left(y_i - \bar{y}_i\right)^2} \tag{17}$$

$$PRSE = 100 \cdot \frac{SE(P)}{P} \tag{18}$$

$$AIC = -2\ln(L) + 2p \tag{19}$$

where y_i is the *observed value*, $\hat{y}_i$ is the *predicted value*, $\bar{y}_i$ is *the mean value*, n is *the number of samples*, p is the *number of parameters*, L is the *likelihood of the fitted model*, P is the *parameter estimate*, and SE(P) is the *parameter standard error*.

Collinearity and heteroscedasticity are common issues in statistical models, in particular when plant traits are considered to be highly correlated. Our approach included the a priori definition of shrub (BV) geometries, calculated using one or more different plant variables. The goal was to identify geometries most suitable for biomass predictions. It is therefore important to note that we do not infer the effect of the variables used, which can be biased by collinearity. Considering the goodness of fit of the cross-validation, we selected those models that demonstrated to be most accurate in predicting the biomass of shrubs to which the model was not fitted, thus demonstrating both the practical usability and uncertainties of the models and associated shrub geometries presented.

Analyses were carried out using R version 4.2.3. (R Core Team 2023), using the *lme4* package (Bates et al. 2015) for linear mixed effects modelling.

Results

Species-specific AGB models

The species-specific equations varied widely in model errors, which ranged from 30.4 to 86.1% in MAPE (Table 2). The highest MAPEs were found in species such as *B. linearis*, *K. oblonga*, *A. dentata*, and *A. chilensis*, while the lowest MAPE was found in *M. obtusa*. R^2 also ranged widely, from 0.851 to 0.429, consistent with the wide range in MAPE. In none of the fourteen species analysed, the performance of the model in RMSE and PRSE improved by adding covariates such as HT and NS (Table 2). The inclusion of HT was suitable only as a combined variable (DCH^2HT) in three out of the fourteen species analysed, but HT as an additional single covariate was not present in any of the best species-specific models, as was also the case with NS. WD was found not to enhance AGB predictions in the preliminary analysis and was not included as a covariate in the model list (see Annex 1). In the Cortaderal site, seven shrub species

Table 2 The best total AGB models found for each shrub species at Cortaderal and Miraflores sites. While the RMSE, MAPE and R^2 are based on a repeated k-fold cross-validation, the correction factor and parameter estimates are given for a fit to the complete data

Species	Model	Parameter estimates (with PRSE in %)		Cross-validation based model performance			
		β_0	β_1	CF	RMSE (kg)	MAPE (%)	R^2
Cortaderal							
A. chilensis	$Y = \beta_0 BV_5^{\beta_1}$	1.887 (22.7)	0.585 (16.5)	1.25	2.25 ± 0.1	86.1 ± 5.9	0.442
A. dentata	$Y = \beta_0 (DCH^2HT)^{\beta_1}$	0.177 (16.9)	0.727 (10.6)	1.28	3.38 ± 0.1	84.2 ± 2.6	0.588
*B. linearis**	$Y = \beta_0 BV_5^{\beta_1}$	3.759 (7.6)	0.740 (6.8)	1.22	1.94 ± 0.1	71.8 ± 1.2	0.736
B. macraei	$Y = \beta_0 BV_1^{\beta_1}$	2.086 (11.2)	0.675 (12.0)	1.08	1.06 ± 0.1	37.8 ± 1.5	0.734
B. horrida	$Y = \beta_0 BV_4^{\beta_1}$	1.030 (606.1)	0.750 (14.3)	1.10	0.16 ± 0.0	40.3 ± 1.9	0.820
E. pulverulenta	$Y = \beta_0 BV_6^{\beta_1}$	1.451 (18.5)	0.920 (5.8)	1.07	1.21 ± 0.1	34.4 ± 1.2	0.811
G. foliosa	$Y = \beta_0 BV_1^{\beta_1}$	2.499 (10.2)	1.001 (7.4)	1.13	2.82 ± 0.4	50.6 ± 2.8	0.789
K. oblonga	$Y = \beta_0 (DCH^2HT)^{\beta_1}$	0.155 (15.1)	0.687 (10.9)	1.25	1.25 ± 0.1	75.5 ± 7.5	0.810
L. hirsuta	$Y = \beta_0 (DCH^2HT)^{\beta_1}$	0.561 (41.1)	0.422 (12.9)	1.05	1.10 ± 0.1	31.1 ± 2.1	0.614
M. obtusa	$Y = \beta_0 BV_4^{\beta_1}$	3.402 (5.3)	0.919 (4.2)	1.05	3.14 ± 0.1	30.4 ± 1.4	0.851
T. bicolor	$Y = \beta_0 CA_e^{\beta_1}$	0.198 (10.3)	0.443 (19.4)	1.05	0.03 ± 0.0	32.4 ± 1.3	0.488
Miraflores							
C. salicifolia	$Y = \beta_0 BV_2^{\beta_1}$	4.297 (6.4)	0.809 (10.0)	1.09	6.33 ± 0.5	41.6 ± 1.9	0.604
P. mitiqui	$Y = \beta_0 CA_c^{\beta_1}$	1.308 (39.5)	0.727 (12.6)	1.09	1.36 ± 0.1	42.3 ± 2.0	0.472
R. trinervia	$Y = \beta_0 BV_3^{\beta_1}$	8.103 (10.2)	0.366 (26.7)	1.11	8.12 ± 0.4	46.0 ± 2.2	0.429

Y = *response variable as total AGB* (aboveground biomass; kg), BV = *bulk volume* (1, 2, 3, 4, 5 and 6 values are specified in Fig. 2; m^3), CA = *crown area* (c = circle and e = ellipse; m^2), DCH = *diameter at collar height* (cm), HT = *total height* (m), NS = *number of stems*, β_0 and β_1 = *model parameters estimated by log–log ordinary least squares and their percent relative standard error PRSE (%)*, R^2 = *coefficient of determination*, CF = *correction factor*, RMSE (kg) = *root mean square error* and MAPE (%) = *mean absolute percentage error*

**B. linearis* was the only species found in both sites, with 42 individuals at Cortaderal and 25 in Miraflores. Therefore, the models included 67 individuals as a single model

(*A. chilensis*, *B. linearis*, *B. macraei*, *B. horrida*, *E. pulverulenta*, *G. foliosa*, and *M. obtusa*) were based only on one covariate, using the BV as the explanatory variable that was found to be the best. On the other hand, the best model in *T. bicolor* was also found based on only one covariate, using the elliptical area (CA_e) as the best explanatory variable. For the other three species presented in the Cortaderal site (*A. dentata*, *K. oblonga*, and *L. hirsuta*), the combined variable (DCH^2HT) was the best predictor for total AGB (Table 2). However, the MAPEs in two of these species were relatively high, with 84.2% in *A. dentata* and 75.5% in *K. oblonga*, respectively. At the Miraflores site, the best model for two species, *C. salicifolia* and *R. trinervia*, had the BV as the best explanatory variable to predict AGB (Table 2). In *P. mitique*, the best model was based on a circle area (CA_c), being the model of choice, also based on a single covariate. The full list of the twenty-nine equations and accuracy metrics for the 14 species-specific models is available in Annex 1, including the nine models that used WD as an additional covariate that was only used during the preliminary analysis.

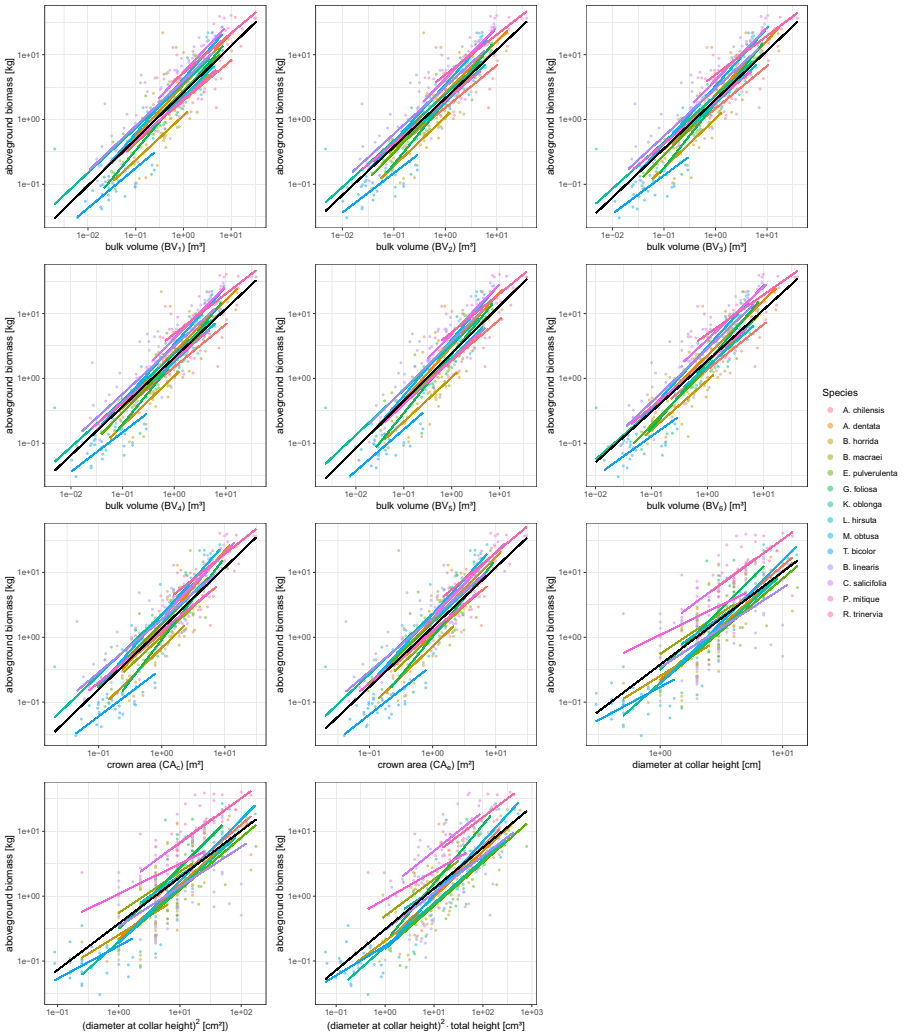

Fig. 4 General relationships between total AGB and BV estimates BV_1, BV_2, BV_3, BV_4, BV_5, BV_6, CA estimates CA_c, CA_e, DCH, its quadratic form DCH^2 and its product with height DCH^2HT

General shrub AGB model

We fitted eleven general AGB models, including species identity as a random effect, to take variance attributable to species identity into account (Fig. 4). The model using BV estimates based on an inverted truncated cone (BV_3) calculated by DCH, CD, and HT had the lowest cross-validation-based RMSE (3.54 kg) and MAPE (54.3%) (Table 3). The alternative models had markedly worse performance ($\Delta AIC > 15$), with the model based on BV_4, which represents an elliptical cube shape, providing the second-best overall results. In general, BV estimates were found to be better general predictors for

Table 3 The results of the general shrub AGB modelling, each representing a linear mixed effect models, which included species identity as random effect. The marginal R^2 indicates the variance explained by the fixed effects, ignoring species identity, whereas the conditional R^2 indicates the variance explained by the entire model, considering species identity. Model performance was assessed and can be compared by AIC based on maximum likelihood fit as well as RMSE and MAPE based on k-fold cross-validation. Parameter uncertainty can be assessed by the PRSE (%), also based on k-fold cross-validation

Model	Parameter estimates (with PRSE in %)		Model performance when fitted to all data					Cross-validation based model performance
	β_0	β_1	R^2 (marg.)	R^2 (cond.)	AIC	CF	RMSE (kg)	MAPE (%)
$Y = \beta_0 BV_1^{\beta_1}$	2.609 (15.2)	0.718 (5.1)	0.71	0.86	743.4	1.16	3.74 ± 0.15	57.5 ± 0.73
$Y = \beta_0 BV_2^{\beta_1}$	2.133 (18.3)	0.748 (5.3)	0.71	0.86	735.2	1.16	3.65 ± 0.16	55.8 ± 0.74
$Y = \beta_0 BV_3^{\beta_1}$	2.024 (20.1)	0.755 (5.5)	0.71	0.87	707.3	1.15	3.54 ± 0.16	54.3 ± 0.74
$Y = \beta_0 BV_4^{\beta_1}$	2.090 (18.7)	0.753 (5.3)	0.71	0.87	725.6	1.15	3.65 ± 0.15	55.0 ± 0.70
$Y = \beta_0 BV_5^{\beta_1}$	2.434 (16.3)	0.732 (5.1)	0.71	0.87	722.4	1.15	3.73 ± 0.18	57.0 ± 0.72
$Y = \beta_0 BV_6^{\beta_1}$	1.873 (23.0)	0.785 (5.4)	0.69	0.86	732.6	1.16	3.79 ± 0.26	58.2 ± 0.74
$Y = \beta_0 CA_c^{\beta_1}$	1.370 (47.8)	0.939 (6.0)	0.69	0.86	748.8	1.16	3.94 ± 0.17	59.1 ± 0.80
$Y = \beta_0 CA_e^{\beta_1}$	1.436 (39.6)	0.923 (5.5)	0.69	0.85	787.0	1.18	4.04 ± 0.19	61.4 ± 0.88
$Y = \beta_0 DCH^{\beta_1}$	0.378 (23.6)	1.432 (8.8)	0.50	0.74	1026.8	1.35	5.02 ± 0.18	116.2 ± 1.81
$Y = \beta_0 DCH^{2\beta_1}$	0.378 (23.6)	0.716 (8.8)	0.50	0.74	1026.8	1.35	5.00 ± 0.17	116.2 ± 1.76
$Y = \beta_0 (DCH^2 HT)^{\beta_1}$	0.309 (20.1)	0.630 (8.2)	0.56	0.79	960.8	1.29	4.23 ± 0.11	95.1 ± 1.30

Y = *response variable as total AGB* (aboveground biomass; kg), BV = *bulk volume* (1, 2, 3, 4, 5 and 6 values are specified in Fig. 2; m^3), CA = *crown area* (c = circle and e = ellipse; m^2), DCH = *diameter at collar height* (cm), HT = *total height* (m), β0 and β1 = *model parameters estimated by log–log ordinary least squares and their percent relative standard error PRSE (%)*, R^2 (marg.) = *marginal coefficient of determination*, R^2 (cond.) = *conditional coefficient of determination*, AIC = *Akaike information criterion*, CF = *correction factor*, RMSE (kg) = *root mean square error* and MAPE (%) = *mean absolute percentage error*

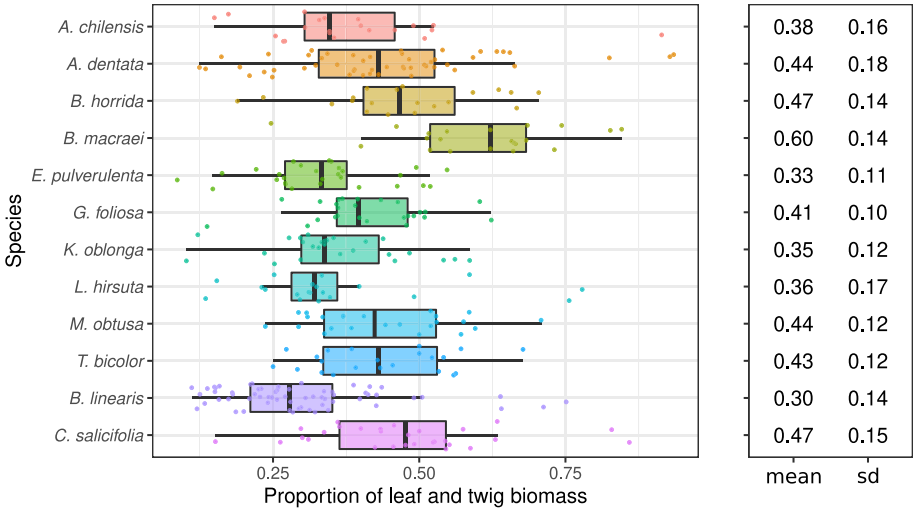

Fig. 5 Boxplots indicating the variability in the proportion of leaf and twig biomass according to shrub species

total AGB than CA or DCH. Models solely based on classical attributes such as DCH and HT exceeded 90% in the cross-validation based mean average prediction error.

Biomass allocation

The relative allocation of biomass to the woody and leaf + twig components varied by species (Fig. 5). Some, such as *B. linearis* (70%), *E. pulverulenta* (67%), and *K. oblonga* (65%), had higher proportions of WB. Only one species, *B. macraei*, had the opposite pattern, with 60% of its total biomass in leaves and twigs.

Discussion

Species-specific AGB models

CA and BV were highly effective predictors in our models, indicating that crown size is more important for shrub AGB prediction than measurements used for trees such as stem diameter (Paton et al. 2002), as reported in most previous studies (Ludwig et al. 1975; Hierro et al. 2000; Blanco Oyonarte and Navarro Cerrillo 2003; Tian et al. 2014; Huff et al. 2017; Flade et al. 2020; Yao et al. 2021). Among the few studies reporting different results, Chen et al. (2023) found that HT, DCH, or the combined variable (DCH^2HT) were the best predictors in most of the equations. According to these authors, species that exhibited weak fits using CA and BV were mostly small trees, while our study focused exclusively on shrubs. Manolis et al. (2016) found that estimating AGB by DBH as explanatory-variable was an accurate predictor for multiple sprouting oak trees in the Mediterranean area. While short multi-stemmed trees (such oaks) are integral to the Mediterranean shrubland landscape, their architectural structure can significantly differ from that of shrub species.

Consequently, allometric equations developed for multi-stemmed trees may prove inadequate when applied to shrubs in the Mediterranean region.

Our study stands out among the few that have compared various geometric crown shapes to estimate BV. Although De Cáceres et al. (2019) did not consider alternative geometric shapes to calculate BV, because authors suggested that this approach often leads to proportional values in β_0 (Usó et al. 1997), but it depends on the specific morphology of the shrub species. For this reason, other authors (e.g., Ludwig et al. 1975; Yao et al. 2021), who tested shapes such as the inverted cone, circular and elliptical cylinders, and hemispherical shapes found good fits for the inverted cone. However, Paton et al. (2002) suggested that complex forms do not provide major improvements through coefficients of determination in log–log equations, probably because they deviate from the current shape/architecture of the shrubs. Our results identified differences in error metrics among the six different geometric shapes, but, for most species, the inverted cone was the best shape, indicating that this shrub geometry is among the most prevalent and useful for species-specific prediction of biomass.

In addition to CA or BV, none of the models improved with the inclusion of additional covariates such as HT or NS. Therefore, our findings illustrate that the addition of other single covariates does not necessarily improve the prediction of shrub biomass. Considering that the estimates of BV originate from calculations already including measurements on shrub HT, CD and DCH, this is not surprising. But it demonstrates that measurements of CA, e.g. by remote sensing, can provide a good alternative to the other more measurement intensive approaches depending on measurements of HT and DCH.

Models of only a few species, *A. dentata*, *K. oblonga*, and *L. hirsuta*, gave slightly better results using the combined explanatory variable DCH^2HT instead of crown-related variables (CA or BV). Similar findings were previously reported by other authors, such as Liu et al. (2015) and Chen et al. (2023), who suggest using this combined variable as a predictor for shrub AGB. However, the model performances for these species were low in general, with a MAPE of 84.2% for *A. dentata* and 75.5% for *K. oblonga*.

General AGB models

As expected, general AGB models, which were applied to very diverse shrub species, showed higher RMSE and MAPE and lower R^2 than most of the species-specific models (with the exception of four species such as *A. chilensis*, *A. dentata*, *B. linearis*, and *K. oblonga* that shower higher MAPE compared to the best general model – BV_3), This effect of species-specific models becoming more tailored to the specific characteristics of each species was already demonstrated by Buech and Rugg (1989) and is in line with more recent studies (e.g., Annighöfer et al. 2016). Thus, the slightly worse performance of general models is likely due to large inter-specific variation in trait-AGB relationships, which cannot be captured so well in one model as in separate species-specific models. Despite this disadvantage, when species-specific biomass models are not available, or species information is not available, generic allometric models can provide a cost-effective prediction of stand-level AGB (Návar et al. 2004; Paul et al. 2016). In addition, to date, models based on remote sensing estimation of AGB cannot employ species-specific information, and therefore only generalized biomass models can be applied for their calibration using ground AGB data (Yang et al. 2017; Bayen et al. 2020; Flade et al. 2020; Menéndez-Miguélez et al. 2022). We consider our general models to be suitable for stand-level biomass estimation.

According to our model evaluation, the six best general models were all based on BV. The next-best models were based on CA and then on the combined variable and DCH. Our findings confirm, as with the species-specific models, that models based on crown attributes are more effective than the classical stem diameter measurements, which are often made on trees. Our results were in line with those of Conti et al. (2019), who have suggested that DCH, CD, and HT can be combined to provide robust AGB estimates of individual shrub species. On the other hand, although the best models came out with BV as the best predictor variable, CA also gave satisfactory results (Table 3). The advantage of the CA is that currently there are several satellite images available (e.g., Chen et al. 2018) in which the shrub crown can be segmented and therefore their area can be estimated, allowing us to estimate their biomass without the need to recognise the shrub species.

Overall, if no detailed information on shrub species identity or shrub geometries is available, but measurements on HT, CD and DCH, then the inverted cone geometry BV_3 can be used to estimate shrub volume and with this finally shrub biomass. Alternatively, direct measurements of shrub volume can be applied to the general biomass models using BV_3. If, however, only measurements of CA are available, the CA_c model can provide AGB estimates with a mean average prediction error of 59%, which is only 5% higher than estimates with the best model based on BV_3. On the other hand, the disadvantage of using BV_3 lies in the measurement of the DCH, while BV_2 models do not require this measurement as an alternative, resulting in only 1.5% higher error estimates compared to BV_3.

Stem, and leaf + twig biomass

Our results in the studied Mediterranean species indicated higher proportions of WB than LTB in 11 of the 12 shrub species, in agreement with Návar et al. (2004) and Tian et al. (2014). Navarro Cerrillo and Blanco Oyonarte (2006) found that the proportion of leaves for some Mediterranean shrub species was between 15 and 21% of the total AGB. However, in most of species investigated in our study, more than one-third of the biomass was made up of elements with a diameter of less than 1 cm (i.e. leaves and twigs). This proportion is certainly influenced by the threshold we used (1 cm, as suggested by Wang and Niu 2016), which was different from other studies (Murray and Jacobson 1982; Sağlam et al. 2008; Huff et al. 2017; De Cáceres et al. 2019) and influenced by the age and height of the individuals and community concerned (Armand et al. 1993; Navarro Cerrillo and Blanco Oyonarte 2006; Vega et al. 2022). In any case, our results highlight that a large part of the shrub biomass was made up of small parts with high flammability, such as *B. macraei*, *B. horrida*, and *C. salicifolia*. Estimating the biomass of leaves and twigs is crucial, especially in the central part of Chile, where wildfires of high severity are common (De la Barrera et al. 2018). Therefore, the information provided in this study is fundamental for quantifying the mean proportion of fine biomass in total fuel load and assessing fire risk in dry shrublands in Chile.

Conclusions

This study provides new species-specific and general allometric equations to estimate AGB for 14 shrub species in Mediterranean-type shrublands in Central Chile, for which such models are scarce. In particular, specific models should be preferred for detailed and species-specific studies, while general models are suitable for stand-level biomass estimates,

including those based on information derived from remote sensing. Our models tested various predictors for shrub AGB estimates, thereby contributing to the field of shrub biomass modelling, which has been largely understudied in comparison to the extensive research on allometric equations for tree biomass estimates. Our study showed that crown dimension (mostly BV) is the best predictor for Mediterranean shrub biomass, with the inverted truncated cone as the best shape for both several species individually and for the general model. Only for a few species, the CA model performs as the best. This information is essential for land managers, ecologists, forest modellers interested in assessing shrubland carbon stock, and fire modellers for assessing fuel loads in fire-prone environments.

Supplementary Information The online version contains supplementary material available at https://doi.org/10.1007/s11056-024-10081-7.

Acknowledgements This study was part of the project GEF entitled "Sistema Integrado de Monitoreo de Ecosistemas Forestales Nativos", GCP/CHI/032/GFF, funded by the Global Environment Facility, the Food and Agriculture Organization of the United Nations and the Ministry of Agriculture of Chile. We wish to thank Marcelo Cárcamo, Diego Muñoz and Mario San Martin for their great contribution to the field data collection and to Dr. Víctor Gerding for reviewing several drafts of this manuscript. Our sincere thanks to the landowners for the willingness to collaborate and provide access to both sites of the study area. Our gratitude to CONAF for the assistance in the field prospection. The corresponding author was supported by CONICYT Doctoral scholarship and by the Fondazione Cassa di Risparmio di Padova e Rovigo (CARIPARO).

Author contributions EK and MZ wrote the paper, MZ and EK performed the statistical analysis, fitted and validated the models, JGu carried out the field measurements, JGa designed the field experiment, YR obtained the grant and coordinated the project, EK, MZ, JGa, FP, DC and RM analysed the results and reviewed the manuscript, MO revised the English grammar and style. All the authors contributed to improve and approved the final version of the paper.

Declarations

Conflict of interest The authors declare no competing interests.

References

Ali A, Xu MS, Zhao YT, Zhang QQ, Zhou LL, Yang XD, Yan ER (2015) Allometric biomass equations for shrub and small tree species in subtropical China. Silva Fenn 49(4):1–10. https://doi.org/10.14214/sf.1275

Alvarez E, Duque A, Saldarriaga J, Cabrera K, de las Salas G, del Valle I, Lema A, Moreno F, Orrego S, Rodríguez L (2012) Tree above-ground biomass allometries for carbon stocks estimation in the natural forests of Colombia. For Ecol Manage 267:297–308. https://doi.org/10.1016/j.foreco.2011.12.013

Annighöfer P, Ameztegui A, Ammer C, Balandier P, Bartsch N, Bolte A, Coll L, Collet C, Ewald J, Frischbier N, Gebereyesus T, Haase J, Hamm T, Hirschfelder B, Huth F, Kändler G, Kahl A, Kawaletz H, Kuehne C, Lacointe A, Lin N, Löf M, Malagoli P, Marquier A, Müller S, Promberger S, Provendier D, Röhle H, Sathornkich J, Schall P, Scherer-Lorenzen M, Schröder J, Seele C, Weidig J, Wirth C, Wolf H, Wollmerstädt J, Mund M (2016) Species-specific and generic biomass equations for seedlings and saplings of European tree species. Eur J Forest Res 135:313–329. https://doi.org/10.1007/s10342-016-0937-z

Armand D, Etienne M, Legrand C, Marechal J, Valette JC (1993) Phytovolume, phytomasse et relations structurales chez quelques arbustes méditerranéens. Ann Sci for 50:79–89. https://doi.org/10.1051/forest:19930106

Baskerville GL (1972) Use of logarithmic regression in the estimation of plant biomass. Can J for Res 2(1):49–53. https://doi.org/10.1139/x72-009

Bates D, Mächler M, Bolker B, Walker S (2015) Fitting linear mixed-effects models using lme4. J Stat Softw 67(1):1–48. https://doi.org/10.18637/jss.v067.i01

Bayen P, Noulèkoun F, Bognounou F, Lykke AM, Djomo A, Lamers JPA, Thiombiano A (2020) Models for estimating aboveground biomass of four dryland woody species in Burkina Faso. West Afr J Arid Environ 180:104205. https://doi.org/10.1016/j.jaridenv.2020.104205

Blanco Oyonarte P, Navarro Cerrillo RM (2003) Aboveground phytomass models for major species in shrub ecosystems of western Andalusia. Forest Syst 12(3):47–55. https://doi.org/10.5424/1078

Buech RR, Rugg DJ (1989) Biomass relations of shrub components and their generality. For Ecol Manage 26(4):257–264. https://doi.org/10.1016/0378-1127(89)90086-8

Caldentey J (1995) Acumulación de biomasa en rodales naturales de *Nothofagus pumilio* en Tierra del Fuego, Chile. Forest Syst 4(2):166–175. https://doi.org/10.5424/544

Chapin FS, Matson PA, Vitousek PM (2011) Principles of terrestrial ecosystem ecology, 2nd edn. Springer, New York, USA, p 529. https://doi.org/10.1007/978-1-4419-9504-9

Chave J, Andalo C, Brown S, Cairns MA, Chambers JQ, Eamus D, Fölster H, Fromard F, Higuchi N, Kira T, Lescure JP, Nelson BW, Ogawa H, Puig H, Riéra B, Yamakura T (2005) Tree allometry and improved estimation of carbon stocks and balance in tropical forests. Oecologia 145:87–99. https://doi.org/10.1007/s00442-005-0100-x

Chen W, Zhao J, Cao C, Tian H (2018) Shrub biomass estimation in semi-arid sandland ecosystem based on remote sensing technology. Conserv Ecol 16:e00479. https://doi.org/10.1016/j.gecco.2018.e00479

Chen J, Fang X, Wu A, Xiang W, Lei P, Ouyang S (2023) Allometric equations for estimating biomass of natural shrubs and young trees of subtropical forests. New for. https://doi.org/10.1007/s11056-023-09963-z

CIREN (1996) Estudio agrológico VI Región. Descripciones de suelos, materiales y símbolos. CIREN publication N°114. Centro de Información de Recursos Naturales. Santiago, Chile, p 479

CONAF (2021) Catastro de los recursos vegetacionales nativos de Chile. Actualizaciones al año 2020. Corporación Nacional Forestal. Santiago, Chile, p 71

Conti G, Díaz S (2013) Plant functional diversity and carbon storage – an empirical test in semi-arid forest ecosystems. J Ecol 101:18–28. https://doi.org/10.1111/1365-2745.12012

Conti G, Enrico L, Casanoves F, Díaz S (2013) Shrub biomass estimation in the semiarid Chaco forest: a contribution to the quantification of an underrated carbon stock. Ann for Sci 70:515–524. https://doi.org/10.1007/s13595-013-0285-9

Conti G, Gorné LD, Zeballos SR, Lipoma ML, Gatica G, Kowaljow E, Whitworth-Hulse JI, Cuchietti A, Poca M, Pestoni S, Fernandes PM (2019) Developing allometric models to predict the individual aboveground biomass of shrubs worldwide. Glob Ecol Biogeogr 28:961–975. https://doi.org/10.1111/geb.12907

Cowling RM, Rundel PW, Lamont BB, Arroyo MK, Arianoutsou (1996) Plant diversity in mediterranean-climate regions. Trends Ecol Evol 11(9):362–366. https://doi.org/10.1016/0169-5347(96)10044-6

Cowling RM, Potts AJ, Bradshaw PL, Colville J, Arianoutsou M, Ferrier S, Forest F, Fyllas NM, Hopper SD, Ojeda F, Procheş Ş, Smith RJ, Rundel PW, Vassilakis E, Zutta BR (2015) Variation in plant diversity in mediterranean-climate ecosystems: the role of climatic and topographical stability. J Biogeogr 42(3):552–564. https://doi.org/10.1111/jbi.12429

Cruz P, Bascuñan A, Velozo J, Rodríguez M (2015) Funciones alométricas de contenido de carbono para quillay, peumo, espino y litre. Bosque 36(3):375–381. https://doi.org/10.4067/S0717-92002015000300005

De Cáceres M, Casals P, Gabriel E, Castro X (2019) Scaling-up individual-level allometric equations to predict stand-level fuel loading in Mediterranean shrublands. Ann for Sci 76:87. https://doi.org/10.1007/s13595-019-0873-4

De la Barrera F, Barraza F, Favier P, Ruiz V, Quense J (2018) Megafires in Chile 2017: Monitoring multiscale environmental impacts of burned ecosystems. Sci Total Environ 637–638:1526–1536. https://doi.org/10.1016/j.scitotenv.2018.05.119

Fick SE, Hijmans RJ (2017) WorldClim 2: new 1-km spatial resolution climate surfaces for global land areas. Int J Climatol 37(12):4302–4315. https://doi.org/10.1002/joc.5086

Flade L, Hopkinson C, Chasmer L (2020) Allometric equations for shrub and short-stature tree aboveground biomass within boreal ecosystems of Northwestern Canada. Forests 11(11):1207. https://doi.org/10.3390/f11111207

Gratani L, Varone L, Ricotta C, Catoni R (2013) Mediterranean shrublands carbon sequestration: environmental and economic benefits. Mitig Adapt Strateg Glob Change 18:1167–1182. https://doi.org/10.1007/s11027-012-9415-1

Hierro JL, Branch LC, Villarreal D, Clark KL (2000) Predictive equations for biomass and fuel characteristics of Argentine shrubs. J Range Manage 53:617–621. https://doi.org/10.2307/4003156

Huang C, Feng C, Ma Y, Liu H, Wang Z, Yang S, Wang W, Fu S, Chen HYH (2022) Allometric models for aboveground biomass of six common subtropical shrubs and small trees. J for Res 33(1317–13):28. https://doi.org/10.1007/s11676-021-01411-y

Huff S, Ritchie M, Temesgen H (2017) Allometric equations for estimating aboveground biomass for common shrubs in northeastern California. For Ecol Manage 398:48–63. https://doi.org/10.1016/j.foreco.2017.04.027

INFOR (2022) Chilean statistical. Yearbook of Forestry. Statistical bulletin N°187. Instituto Forestal. Santiago, Chile, p 256

Kouamé YAG, Millan M, N'Dri AB, Charles-Dominique T, Konan M, Bakayoko A, Gignoux J (2022) Multispecies allometric equations for shrubs and trees biomass prediction in a Guinean savanna (West Africa). Silva Fenn 56(2):10617. https://doi.org/10.14214/sf.10617

Kutchartt E, Gayoso J, Pirotti F, Bucarey A, Guerra J, Hernández J, Corvalán P, Drápela K, Olson M, Zwanzig M (2021) Aboveground tree biomass of *Araucaria araucana* in southern Chile: measurements and multi-objective optimization of biomass models. iForest 14:61–70. https://doi.org/10.3832/ifor3492-013

Kutchartt E, Gayoso J, Guerra J, Pirotti F, Castagneri D, Anfodillo T, Rojas Y, Olson M, Zwanzig M (2022) Basic wood density and moisture content of 14 shrub species under two different site conditions in the Chilean Mediterranean shrubland. Forest Syst 31(1):eSC01. https://doi.org/10.5424/fs/2022311-18160

Liu Z, Chen R, Song Y, Han C, Yang Y (2015) Estimation of aboveground biomass for alpine shrubs in the upper reaches of the Heihe River Basin, Northwestern China. Environ Earth Sci 73:5513–5521. https://doi.org/10.1007/s12665-014-3805-5

Ludwig JA, Reynolds JF, Whitson PD (1975) Size-biomass relationships of several Chihuahuan desert shrubs. Am Midl Nat 94(2):451–461. https://doi.org/10.2307/2424437

Lübert F, Pliscoff P (2018) Sinopsis bioclimática y vegetacional de Chile. Editorial Universitaria, Santiago, Chile, p 384

Madrigal-González J, Fernández-Santos B, Silla F, García Rodríguez JA (2023) Shrub diversity in Mediterranean shrublands: rescuer or victim of productivity? J Veg Sci 34(1):e13169. https://doi.org/10.1111/jvs.13169

Manolis EN, Zagas TD, Poravou CA, Zagas DT (2016) Biomass assessment for sustainable bioenergy utilization in a Mediterranean forest ecosystem in northwest Greece. Ecol Eng 91:537–544. https://doi.org/10.1016/j.ecoleng.2016.02.041

Matula R, Damborská L, Nečasová M, Geršl M, Šrámek M (2015) Measuring biomass and carbon stock in resprouting woody plants. PLoS ONE 10(2):e0118388. https://doi.org/10.1371/journal.pone.0118388

Médail F, Quézel P (1999) Biodiversity hotspots in the Mediterranean Basin: setting global conservation priorities. Conserv Biol 13(6):1510–1513

Menéndez-Miguélez M, Calama R, Del Río M, Madrigal G, López-Senespleda E, Pardos M, Ruiz-Peinado R (2022) Species-specific and generalized biomass models for estimating carbon stocks of young reforestations. Biomass Bioenergy 161:106453. https://doi.org/10.1016/j.biombioe.2022.106453

Miranda (2022) Bosques y matorrales de la zona central: La urgente necesidad de proteger los ecosistemas de transición. Fundación Terram. Santiago, Chile, p 52

Murray RB, Jacobson MQ (1982) An evaluation of dimension analysis for predicting shrub biomass. J Range Manage 35(4):451–454. https://doi.org/10.2307/3898603

Myers N, Mittermeier RA, Mittermeier CG, da Fonseca GAB, Kent J (2000) Biodiversity hotspots for conservation priorities. Nature 403:853–858. https://doi.org/10.1038/35002501

Návar J, Méndez E, Nájera A, Graciano J, Dale V, Parresol B (2004) Biomass equations for shrub species of Tamaulipan thornscrub of North-eastern Mexico. J Arid Environ 59:657–674. https://doi.org/10.1016/j.jaridenv.2004.02.010

Navarro Cerrillo RM, Blanco Oyonarte P (2006) Estimation of above-ground biomass in shrubland ecosystems of southern Spain. Forest Syst 15(2):197–207. https://doi.org/10.5424/srf/2006152-00964

Northup BK, Zitzer SF, Archer S, McMurtry CR, Boutton TW (2005) Above-ground biomass and carbon and nitrogen content of woody species in a subtropical thornscrub parkland. J Arid Environ 62:23–34. https://doi.org/10.1016/j.jaridenv.2004.09.019

Nyamukuru A, Whitney C, Tabuti JRS, Esaete J, Low M (2023) Allometric models for aboveground biomass estimation of small trees and shrubs in African savanna ecosystems. Trees for People 11:100377. https://doi.org/10.1016/j.tfp.2023.100377

Orrego J (2014) Acumulación de biomasa aérea en *Colliguaja odorifera* Mol., *Retanilla trinervia* (Gillies et Hook.) Hook. et Arn. y Berberis antinacantha Mart. en la Reserva Nacional Roblería del Cobre de Loncha. Dissertation, University of Chile

Papió C, Trabaud L (1990) Structural characteristics of fuel components of five Mediterranean shrubs. For Ecol Manage 35:249–259. https://doi.org/10.1016/0378-1127(90)90006-W

Pasalodos-Tato M, Ruiz-Peinado R, del Río M, Montero G (2015) Shrub biomass accumulation and growth rate models to quantify carbon stocks and fluxes for the Mediterranean region. Eur J Forest Res 134:537–553. https://doi.org/10.1007/s10342-015-0870-6

Paton D, Nuñez J, Bao D, Muñoz A (2002) Forage biomass of 22 shrub species from Monfragüe Natural Park (SW Spain) assessed by log-log regression models. J Arid Environ 52:223–231. https://doi.org/10.1006/jare.2001.0993

Paul KI, Roxburgh SH, England JR, Ritson P, Hobbs T, Brooksbank K, Raison RJ, Larmour JS, Murphy S, Norris J, Neumann C, Lewis T, Jonson J, Carter JL, McArthur G, Barton C, Rose B (2013) Development and testing of allometric equations for estimating above-ground biomass of mixed-species environmental plantings. For Ecol Manage 310:483–494. https://doi.org/10.1016/j.foreco.2013.08.054

Paul KI, Roxburgh SH, Chave J, England JR, Zerihun A, Specht A, Lewis T, Bennett LT, Baker TG, Adams MA, Huxtable D, Montagu KD, Falster DS, Feller M, Sochacki S, Ritson P, Bastin G, Bartle J, Wildy D, Hobbs T, Larmour J, Waterworth R, Stewart HTL, Jonson J, Forrester DI, Applegate G, Mendham D, Bradford M, O'Grady A, Green D, Sudmeyer R, Rance SJ, Turner J, Barton C, Wenk EH, Grove T, Attiwill PM, Pinkard E, Butler D, Brooksbank K, Spencer B, Snowdon P, O'Brien N, Battaglia M, Cameron DM, Hamilton S, McAuthur G, Sinclair J (2016) Testing the generality of above-ground biomass allometry across plant functional types at the continent scale. Glob Chang Biol 22(6):2106–2124. https://doi.org/10.1111/gcb.13201

Peichl M, Arain MA (2007) Allometry and partitioning of above- and belowground tree biomass in an age- sequence of white pine forests. For Ecol Manage 253(1–3):68–80. https://doi.org/10.1016/j.foreco.2007.07.003

R Core Team (2023) R: A language and environment for statistical computing, version 4.2.3. The R project for statistical computing. Vienna, Austria. [online] URL: http://www.r-project.org/

Ruiz-Peinado R, Monero G, Juarez E, Montero G, Roig S (2013) The contribution of two common shrub species to aboveground and belowground carbon stock in Iberian dehesas. J Arid Environ 91:22–30. https://doi.org/10.1016/j.jaridenv.2012.11.002

Sah JP, Ross MS, Koptur S, Snyder JR (2004) Estimating aboveground biomass of broadleaved woody plants in the understory of Florida Keys pine forests. For Ecol Manage 203(1–3):319–329. https://doi.org/10.1016/j.foreco.2004.07.059

Sağlam B, Küçük Ö, Bilgili E, Dinç Durmaz B, Baysal I (2008) Estimating fuel biomass of some shrub species (Maquis) in Turkey. Turk J Agric for 32(4):349–356

Schulz JJ, Cayuela L, Echeverria C, Salas J, Rey Benayas JM (2010) Monitoring land cover change of the dryland forest landscape of Central Chile (1975–2008). Appl Geogr 30:436–447. https://doi.org/10.1016/j.apgeog.2009.12.003

Schulz JJ, Cayuela L, Rey-Benayas JM, Schröder B (2011) Factors influencing vegetation cover change in Mediterranean Central Chile (1975–2008). Appl Veg Sci 14:571–582. https://doi.org/10.1111/j.1654-109X.2011.01135.x

Smith-Ramírez C, Grez A, Galleguillos M, Cerda C, Ocampo-Melgar A, Miranda MD, Muñoz AA, Rendón-Funes A, Díaz I, Cifuentes C, Alaniz A, Seguel O, Ovalle J, Montenegro G, Saldes-Cortés A, Martínez-Harms MJ, Armesto JJ, Vita A (2023) Ecosystem services of Chilean sclerophyllous forests and shrublands on the verge of collapse: a review. J Arid Environ 211:104927. https://doi.org/10.1016/j.jaridenv.2022.104927

Tian Y, Jia Z, Yang X (2014) Improving shrub biomass estimations in the Qinghai-Tibet Plateau: age-based Caragana intermedia allometric models. For Chron 90(2):154–160

Tischer A, Zwanzig M, Frischbier N (2020) Spatiotemporal statistics: analysis of spatially and temporally correlated throughfall data: exploring and considering dependency and heterogeneity. In: Levia DF, Carlyle-Moses DE, Iida S, Michalzik B, Nanko K, Tischer A (eds) Forest-water interactions. Ecological studies, vol 240. Springer, Cham. https://doi.org/10.1007/978-3-030-26086-6_8

Usó JL, Mateu J, Karjalainen T, Salvador P (1997) Allometric regression equations to determine aerial biomasses of Mediterranean shrubs. Plant Ecol 132:59–69. https://doi.org/10.1023/A:1009765825024

Vega JA, Arellano-Pérez S, Álvarez-González JG, Fernández C, Jiménez E, Fernández-Alonso JM, Vega-Nieva DJ, Briones-Herrera C, Alonso-Rego C, Fontúrbel T, Ruiz-González AD (2022) Modelling aboveground biomass and fuel load components at stand level in shrub communities in NW Spain. For Ecol Manage 505:119926. https://doi.org/10.1016/j.foreco.2021.119926

Vora RS (1988) Predicting biomass of five shrub species in northeastern California. J Range Manage 41(1):63–65. https://doi.org/10.2307/3898792

Wang S, Niu S (2016) Fuel classes in conifer forests of Southwest Sichuan, China, and their implications for fire susceptibility. Forests 7:52. https://doi.org/10.3390/f7030052

Yang H, Wang Z, Tan H, Gao Y (2017) Allometric models for estimating shrub biomass in desert grassland in northern China. Arid Land Res Manag 31(3):283–300. https://doi.org/10.1080/15324982.2017.1301595

Yao X, Yang G, Wu B, Jiang L, Wang F (2021) Biomass estimation models for six shrub species in hunshandake sandy land in inner Mongolia, northern China. Forests 12:167. https://doi.org/10.3390/f12020167

Zeng HQ, Liu QJ, Feng ZW, Ma ZQ (2010) Biomass equations for four shrub species in subtropical China. J for Res 15:83–90. https://doi.org/10.1007/s10310-009-0150-8

Zianis D, Mencuccini M (2004) On simplifying allometric analyses of forest biomass. For Ecol Manage 187(2–3):311–332. https://doi.org/10.1016/j.foreco.2003.07.007

Authors and Affiliations

Erico Kutchartt[1,2] · Jorge Gayoso[3] · Javier Guerra[4] · Francesco Pirotti[2] · Daniele Castagneri[2] · Radim Matula[5] · Yasna Rojas[6] · Mark E. Olson[7] · Martin Zwanzig[8]

✉ Erico Kutchartt
erico.kutchartt@ctfc.cat

[1] Forest Science and Technology Centre of Catalonia (CTFC), Carretera de Sant Llorenç de Morunys, Km 2, 25280 Solsona, Spain

[2] Department of Land, Environment, Agriculture and Forestry (TESAF), University of Padova, Via dell'università 16, 35020 Legnaro, PD, Italy

[3] Instituto de Bosques y Sociedad (IBOS), Universidad Austral de Chile. Campus Isla Teja, 5090000 Valdivia, Chile

[4] Campo Digital GIS and Remote Sensing, Luxemburgo 1378, 5312081 Osorno, Chile

[5] Department of Forest Ecology, Czech University of Life Sciences Prague, Kamýcká 29, Prague, Czech Republic 16500

[6] Instituto Forestal, Fundo Teja Norte S/N, 5090000 Valdivia, Chile

[7] Instituto de Biología, Universidad Nacional Autónoma de México, Tercer Circuito S/N de Ciudad Universitaria, 04510 Ciudad de Mexico, México

[8] Department of Forest Sciences, Institute of Forest Growth and Forest Computer Sciences, Technische Universität Dresden, Pienner Str. 8, 01737 Tharandt, Germany